Final Report to NOAA MAPP Program (NA11OAR4310102)

Report Period: 09/01/2011 - 08/31/2015 (with a one-year no-cost extension)

Understanding the Emerging Central-Pacific ENSO and Its Impacts on North American Climate

Jin-Yi Yu, Professor
Department of Earth System Science
University of California; Irvine, CA 92697-3100
(Phone) 949-824-3878; (Email): jyyu@uci.edu

SUMMARY

This project proposed data analyses and model experiments to better understand the possibly different impacts of the Central-Pacific (CP) and Eastern-Pacific (EP) types of El Niño-Southern oscillation (ENSO) on North American climate. Specifically, the project sought to answer the following scientific issues: (1) How does the CP ENSO affect the extratropical atmosphere-ocean to impact the North American climate and how does the CP ENSO impact differ from the EP ENSO impact, (2) Are modern climate models capable of simulating the different impacts of these two types of ENSO and what can the two-ENSO view offer for further improvements of the models, and (3) Why has the CP ENSO occurred more frequently in recent decades. We have conducted the proposed research tasks in the past four years and have successfully addressed all these scientific issues. A total of twenty journal papers have been published from this project to report our findings. The results have also been reported in national and international conferences and meetings.

We find from this project that the emerging CP El Niño produces distinct impacts on the US climate from the traditional EP El Niño. The changing impacts on the US climate are identified for winter precipitation and surface temperature patterns, spring stream flow variations in the Mississippi River basin, and summer Great Plain low level jet (GPLJ) strength. The changing impacts make the specific US regions that are most vulnerable to the El Niño influences shifted in recent decades after the El Niño changes type. We find that the emerging CP El Niño events makes US to receive less winter rainfalls since 1990, which could be a contributing factor for the prolonged US drought. The CP El Niño also weakened the summer GPLLJ strength to lead to a drier environment in the central United States. We find that most of the CMIP5 models can capture the impact of the EP El Niño on US but not the impact of the CP El Niño. The cause of this performance difference is identified by examining the relationships among El Niño forcing, outgoing longwave radiation anomalies, and atmospheric wave train pattern. Finally, we are able to prove that the recent emergence of the Central Pacific El Niño is a consequence of the phase change of Atlantic Multi-decadal Oscillation (AMO) but not necessary a consequence of global warming.

In conclusion, we have achieved the goals that we proposed for this project and have obtained a good understanding of the cause of the increased occurrence of the CP ENSO and its impacts on the North American climate. The understanding can be used to improve the predictions of the ENSO impacts on the US climate.

RESULTS AND ACCOMPLISHMENTS

A. Identify the Cause for the Increased Occurrence of the CP ENSO

The recent identification of two distinct types (or flavors) of ENSO offers a new way to consider how ENSO and its impacts may change when the climate changes. These two ENSO types are the EP type that produces sea surface temperature (SST) anomalies near the South America coast and the CP type that produces anomalies near the international dateline. While the EP ENSO used to be the conventional type of ENSO, it has come to people's attention that the CP ENSO has gradually increased its occurrence in the recent two decades. Three of the four El Niño events in the 21st century (the 2002/03, 2004/05, and 2009/10 events) have been CP type. We conducted the following research tasks to understand the cause for the increased occurrence of the CP ENSO.

A1. Using NCEP's CFSR to study the cause of the emergence of the CP El Niño after 1990

We seek to understand the reason why the CP type has occurred more often during the past few decades, particularly since the 1990s. We analyzed NCEP's CFSv2 reanalysis (CFSR) to conclude that the SST variability in the tropical central Pacific was more closely related to the SST variability in the tropical eastern Pacific before 1990 but more closely related to sea level pressure (SLP) variations associated with the North Pacific Oscillation (NPO) after 1990. In the post-1990 period (i.e., 1991-2009), the evolution of the Niño4 SST index is more closely related to and almost in phase with the NPO index but is less related to the Niño3 SST index (Fig. 1). On the contrary, in the pre-1990 period (i.e., 1979-1990), the Niño4 index is more related to and in phase with the Niño3 index but less related to the NPO index.

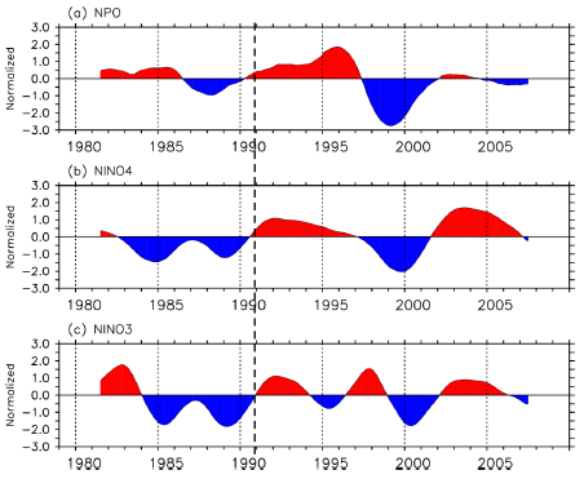

Figure 1. Time series of (a) NPO, (b) Niño 4, and (c) Niño3 indices which are five-year low pass filtered. Values shown are normalized by their standard deviations.

Related to this change, tropical Pacific SST anomalies tend to spread from the eastern to central tropical Pacific before 1990 in a pattern resembling that associated with the EP type of El Niño, but are more closely connected to SST variability in the north subtropical Pacific after 1990 with a pattern resembling that of the CP type of El Niño (Fig. 2). This study concludes that the increased influence of the NPO on the tropical Pacific is likely a reason for the greater frequency of occurrence of the CP El Niño since

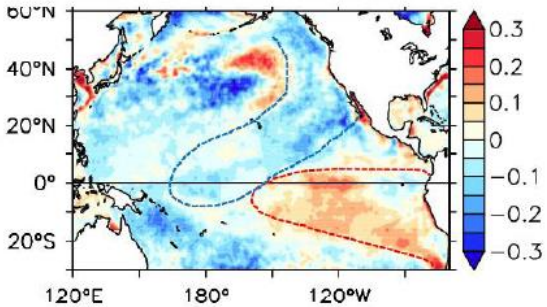

Figure 2. The difference between the standard deviations of SST anomalies calculated from 1979-1990 and those calculated from 1991-2009.

1990. By analyzing the mean atmospheric circulation during these two periods, it is noted that the increased NPO influence is associated with a strengthening Hadley circulation and a weakening Walker circulation after 1990.

A2. <u>A cause for the emergence of the CP ENSO:</u> The phase change of Atlantic Multi-decadal Oscillation (AMO) in 1990s

This study is conducted to further understand why the El Niño shifts from the EP type to the CP type in recent decades. This study was conducted to answer this question. Exciting findings were obtained, and we believe that we have a very good clue for the answer.

While the generation of the EP El Niño involves traditional El Niño dynamics centered on thermocline variations along the equatorial Pacific, we have been arguing that the generation of the CP El Niño is linked to forcing from the extratropical atmosphere. The extratropical atmospheric forcing is suggested to penetrate to the tropical central Pacific through the Pacific Meridional Mode (PMM) via a seasonal footprinting mechanism. Since the CP El Niño has occurred more frequently in recent decades, it is natural to wonder if the PMM has also experienced slow variations, and how are these slow variations, if any, related to the leading decadal variability modes in the Pacific or even the Atlantic, such as the Pacific Decadal Oscillation (PDO) and Atlantic Multidecadal Oscillation (AMO). Statistical analyses are conducted here using observational and re-analysis data since 1948 to answer these two questions.

Since the PMM is a mode of coupled atmosphere-ocean variability, the PMM intenisty can be measured by the coupling strength between SST and surface wind anomalies. We found that the PMM coupling strength has increased during the past four decades in a step-wise manner (Fig. 3), with the first increase around 1976 and the second around 1993. To understand the reason why the PMM coupling strength is different among these three periods, we examined the mean sea level pressure (SLP) in each of the three periods. The 1976-enhancement is found to be accompanied by an intensification of the Aleutian Low and the 1993-enhancement to be accompanied by an intensification of the Pacific Subtropical High. What could be the causes for these decadal SLP changes? On decadal timescales, the PDO and the AMO are two major modes of variability that are capable of influencing global climate. We explore the possible connections between them and the decadal PMM variations. Evidence is found that the 1976-enhancement is related to a phase change in PDO, while the 1993-enhancement is related to a phase change in AMO. The PMM coupling strength was first enhanced around 1976 after when the PDO switched from a negative

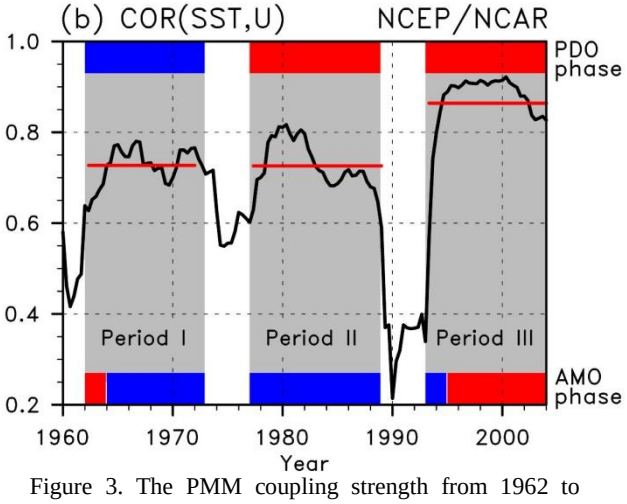

Figure 3. The PMM coupling strength from 1962 to 2005. The gray shading is used to emphasize the three different periods (1962-1972, 1977-1988 and 1993-2004). The shadings on the top and bottom are the positive/negative (red/blue) phases of the 12-year low pass filtered AMO and PDO, respectively.

to positive phase and the Aleutian Low intensified. The intensified low can displace the tropospheric jetstream equatorward and intensify the extratropical influence on the subtropical Pacific Ocean to enhance the PMM. The second enhancement of the PMM coupling occurred around the early-to-middle 1990s when the AMO switched from a negative to positive phase and intensified the Pacific Subtropical High. Therefore, our investigations reveal that the recent emergence of the Central Pacific El Niño is a Pacific Ocean response to the phase change of the AMO.

A3. <u>Pacific-Atlantic Interactions:</u> Linking the recent emergence of CP El Niño to Atlantic Multi-decadal Oscillation (AMO)

The recent shift in El Niño location has posed an interesting challenge to existing theories of El Niño, caused several unexpected changes in global weather and climate patterns (including US climate), and stirred intense activity in the climate research community. Our investigations have enabled us to explain the recent emergence of the CP El Niño via the following chain of events: A switch in the AMO to its positive phase in the early 1990s led to an intensification of the Pacific Subtropical High, likely via an atmospheric teleconnection that involves the poleward displacement of jetstreams over the North Pacific and Atlantic. The intensified High resulted in stronger-than-average background trade winds that enhanced the wind-evaporation-SST (WES) feedback mechanism, strengthening the subtropical Pacific coupling between the atmosphere and ocean, and ultimately leading to increased interannual SST variability in the equatorial central Pacific. Thus, the shift in El Niño to the CP type in recent decades can be understood as a Pacific Ocean response to a phase change in the AMO, and understanding the inter-basin interactions involved in this response will help improve climate predictions in the Pacific Rim including the US.

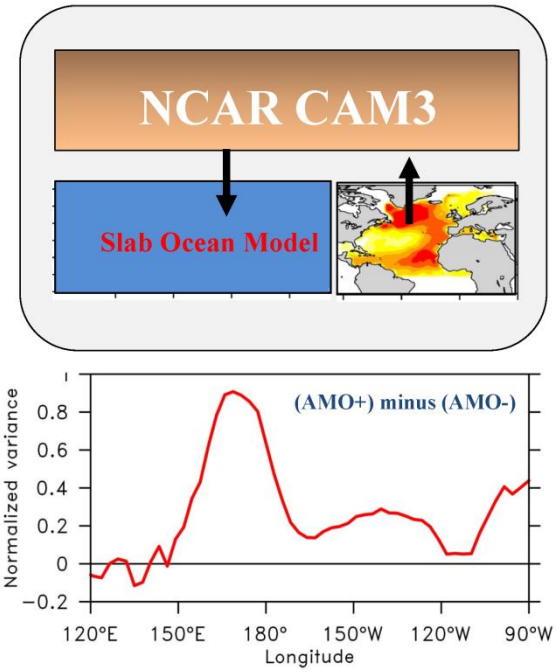

Figure 4. The model design for the CAM3-Slab Ocean model experiment (a) and the differences in the equatorial Pacific SST variability between the AMO(+) and AMO(-) experiments.

We also couple Version 3.1 of the NCAR Community Atmospheric Model (CAM3) to a mixed-layer slab ocean model to demonstrate that the AMO phase change can indeed affect the amplitude of the CP El Niño. Two experiments were conducted (see Figure 3): an AMO-positive phase run and an AMO-negative phase run, in which SSTs corresponding to the positive and negative phases of the AMO were prescribed respectively over the North Atlantic (0°–70°N). SSTs in other regions were predicted using the slab ocean model. The model was integrated for 120 years for each run and only the last 100 years were used for analysis. The SLP differences between the two experiments are characterized by an intensification of the Pacific subtropical high confirming the finding of our observational analyses. We then compared the interannual SST variability between the two runs along the equator (5°S–5°N) during boreal winter (December–

February; DJF) when El Niño typically peaks. We found the largest difference occurs in the central Pacific, where the variability in the AMO-positive run is almost double that in the AMO-negative run (Fig. 4). Therefore, this set of the coupled model experiments further confirms that a switch of the AMO to its positive phase can lead to an increase of SST variability in the tropical central Pacific and increase the occurrence of the CP El Niño.

B. Identify the Different Impacts of the Two Types of ENSO on US Climate

The regional impacts of ENSO on the Pacific Rim have been extensively studied and it is well recognized that North American climate receives considerable influence from ENSO. However, the existence of two types of ENSO was not taken into account in these past studies of ENSO impacts. The classical view of the ENSO impact could be a mixture of impacts from the conventional EP ENSO and the emerging CP ENSO. There are indications that the response can be sensitive to the exact location of the SST anomalies. The increased occurrence of the CP ENSO in the recent decades may change the ENSO impacts on the US climate. This project adopts this two-ENSO view to revise our traditional understanding of the ENSO impacts on North America. We conducted observational analyses and forced atmospheric model experiments to identify the changing impacts on the winter, spring, and summer climate of the US.

B1. <u>The changing impacts of ENSO on US winter temperature:</u> a 90-degree rotation of the impact pattern

We conducted statistical analyses with observational data, numerical experiments with a forced atmospheric general circulation model (AGCM), and case studies with major El Niño events since 1950 to show that the impacts produced by the CP and EP types of El Niño on US winter temperatures are very different. During EP El Niño events, positive winter temperature anomalies are concentrated mostly over the northeastern part of the US and negative anomalies are most obvious over the southwestern states (Fig. 5a). During CP El Niño events, the warm anomalies are located in northwestern US and the cold anomalies are centered in the southeastern US (Fig. 5b). The US temperature impact patterns are

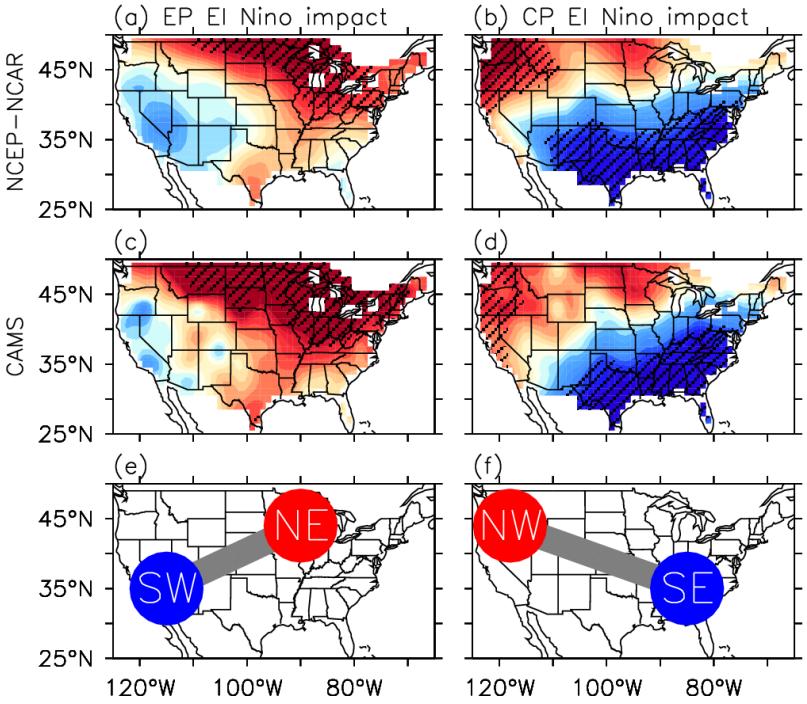

Figure 5. Observed US winter (January-February-March) surface air temperature anomalies regressed onto the (a) EP and (b) CP El Niño indices. Regression coefficients significant at the 90% confidence level based on the student-t test are shaded.

rotated by about 90 degrees between these two types of El Niño. These two impact patterns are able to be reproduced (Figs. 5c and d) in the forced experiments performed with Version 4 of the Community Atmosphere Model (CAM4) from NCAR, in which the SST anomalies of the EP and CP El Niño were separately used to force the model in two different sets of ensemble experiments. The regressed impact patterns can also be identified (not shown) in the four strongest EP El Niño events (1997, 1982, 1972, and 1986 events) and four of the top five strongest CP El Niño events (i.e., the 2009, 1957, 2002, and 2004 events).

We further showed that the cause of the different impacts is the different wave train patterns produced by these two types of El Niño in the extratropical atmosphere. The winter atmosphere produces a Pacific/North American teleconnection (PNA) pattern, which consists of a positive anomaly center extending from eastern Alaska to northwestern US and a negative anomaly center over southeastern US, resulting in a warm-northwest, cold-southeast pattern of temperature anomalies. During the EP El Niño, the winter atmosphere produces a poleward wave train emanating from the tropical eastern Pacific, across the southwestern US, and into the northeastern US, leading to the cold-southwest, warm-northeast pattern in US winter temperatures.

B2. <u>Mechanism for the changing impacts of ENSO on US winter temperature:</u> PNA vs TNH teleconnection patterns

Why would these two types of El Niño produce different impacts on US winter temperatures? A regression analysis with the EP and CP El Niño indices reveals that in association with CP El Niño events (Fig. 6a), the winter atmosphere produces an anomaly pattern of 500mb geopotential height that resembles the Pacific/North American teleconnection (PNA) pattern. This pattern consists of a positive anomaly center extending from eastern Alaska to northwestern US and a negative anomaly center over southeastern US, resulting in a warm-northwest, cold-southeast pattern of temperature anomalies. However, such a PNA-like pattern does not appear in the winter atmosphere during EP El Niño events (Fig. 6b). The anomaly pattern of the 500mb geopotential heights in this case is characterized by a poleward wave train emanating from the tropical eastern Pacific, across the southwestern US, and into the northeastern US, leading to the cold-southwest, warm-northeast pattern in US winter temperatures. This pattern is similar to the so-called Tropical Northern Hemisphere (TNH) pattern.

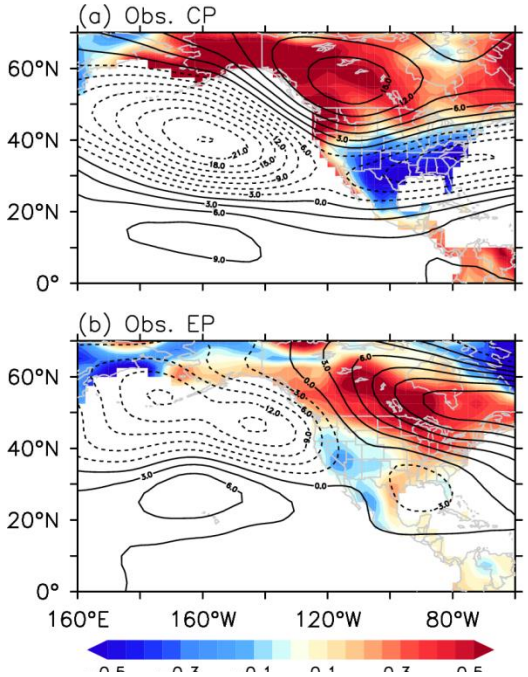

Figure 6. Observed anomalies of the JFM-mean 500mb geopotential heights (contours) and surface air temperatures (color shade) regressed with the (a) CP and (b) EP indices.

Our results demonstrated that the EP and CP types of El Niño have different impacts on US winter surface air temperatures via exciting different teleconnection

patterns in the extratropical atmosphere. Based on this view, the recent emergence of the CP type of El Niño implies that the impact of El Niño on US winter temperature could become more pronounced over the northwestern and southeastern US than any other part of the country. Our results refine the classical view of El Niño impact and provide a framework for more accurate predictions of its effects on the US. Our findings also have important implications on how the El Niño will influence US climate in the future, should the occurrence of the CP type of El Niño continue to rise in response to climate change

B3. <u>Ensemble forced AGCM experiments:</u> Confirming the changing ENSO impacts

To further confirm that the different impacts revealed by the regression analysis are due to the different SST forcing from the two types of El Niño, forced experiments were performed with version 4 of the Community Atmosphere Model (CAM4) from NCAR. Three sets of ensemble experiments were conducted with a T42 (64x128) Euler spectral resolution of CAM4: a control run, an EP run, and a CP run. In the control run, climatological and annually-cycled SSTs are used as the boundary condition to force CAM4. For the EP (CP) run, the CAM4 is forced by SSTs constructed by adding together the climatological SSTs and the SST anomalies of the EP (CP) El Niño. For each of the runs, a 10-member ensemble of 22-month integrations was conducted with the El Niño SST anomalies evolved from the developing phase, peak phase, to decaying phase. The peak phases of the SST anomalies were placed in December of Year 1 of each member. The SST anomalies used in the experiments were constructed by regressing tropical Pacific SST (20°S-20°N) anomalies to the EP and CP El Niño indices and then scaled to typical El Niño magnitudes (shown in Figure 7). During the typical evolution of an EP El Niño event, warm SST anomalies first appear south of the equator, near the South American coast, then extend northward toward the equatorial cold tongue, and eventually spread westward

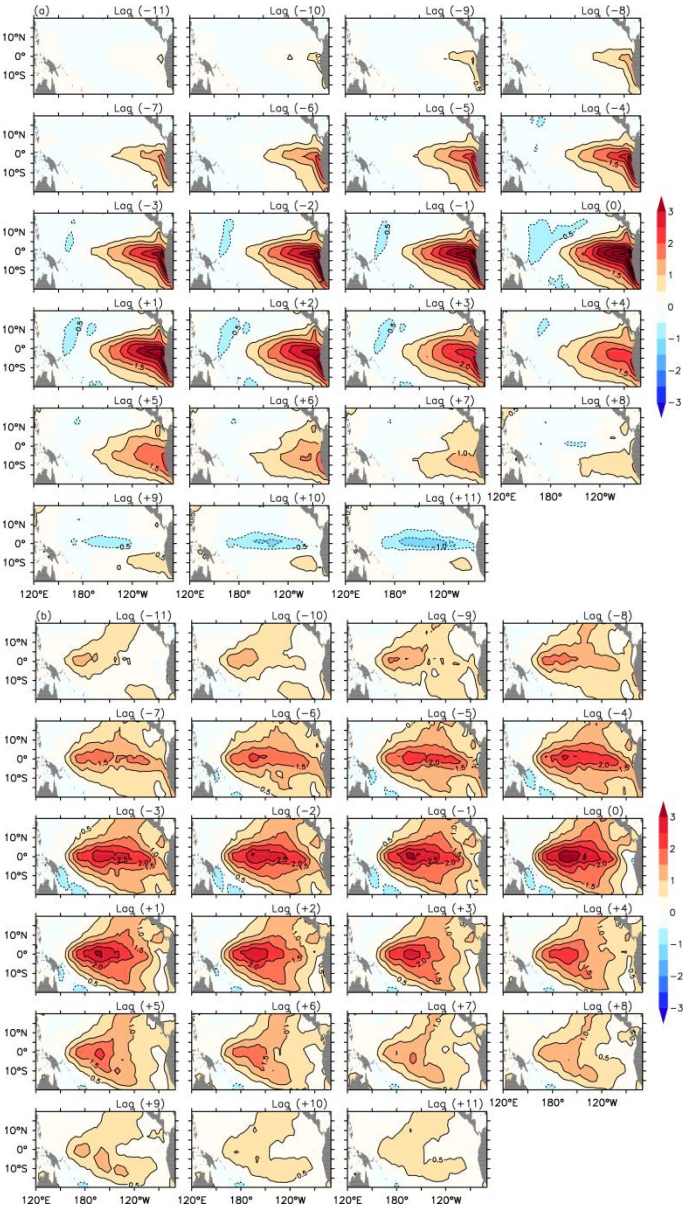

Figure 7. SST anomalies regressed onto the (a) EP and (b) CP El Niño index, from 11 months before to 11 months after the peak of the index. The values shown are the regression coefficients scaled by a factor of 4.5. Contour intervals are 0.5□C.

into the central equatorial Pacific. As for a typical CP El Niño event, the warming appears first in the northeast subtropical Pacific and then extends into the central equatorial Pacific. After SST anomalies have been established at the equator, the warming intensifies rapidly with the anomalies extending eastward, but remaining detached from the South American Coast.

The impacts produced by the EP and CP types of El Niño in the model experiments were identified by subtracting the ensemble mean of the control run from the ensemble means of the EP and CP runs (see Figs. 5c and d). It is very encouraging to find that the regressed winter US impact patterns produced by the EP and CP types of El Niño in the observations were reproduced in the forced model experiments. The CAM4 model produces a warm-northeast, cold-southwest anomaly pattern in surface air temperatures when the model is forced by SST anomalies of the EP El Niño. The same model produces a warm-northwest, cold-southeast anomaly pattern when it is forced by the SST anomalies of the CP El Niño. The centers of the winter temperature anomalies coincide reasonably well with the regression results based on observations.

B4. The changing impact of El Niño on US winter precipitation: An enhanced drying effect of Central-Pacific El Niño on US winter precipitation

In what is arguably one of the most dramatic phenomena possibly associated with climate change or natural climate variability, the location of El Niño has shifted more to the central Pacific in recent decades. In this study, we use statistical analyses, numerical model experiments, and case studies to show that the Central-Pacific El Niño enhances the drying effect, but weakens the wetting effect, typically produced by traditional Eastern-Pacific El Niño events on the US winter precipitation. As a result, the emerging Central-Pacific El Niño produces an overall drying effect on the US winter, particularly over the Ohio-Mississippi Valley, Pacific Northwest, and Southeast. The enhanced drying effect is shown related to a more southward displacement of tropospheric jet streams that control the movements of winter storms.

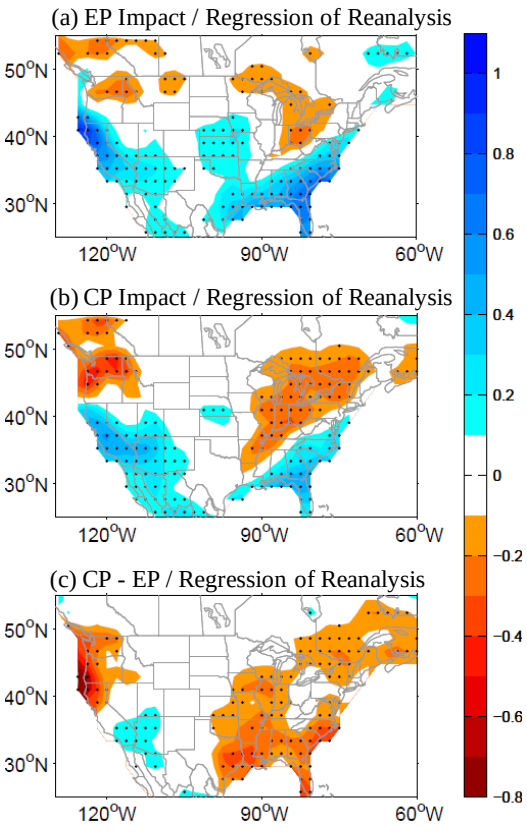

Figure 8. US winter (January-February-March; JFM) precipitation anomalies associated with the (a) EP El Niño, (b) CP El Nino, and (c) the difference between (b) and (a).

We first regress US winter (January-February-March; JFM) precipitation anomalies to the EP and CP El Niño indices to identify the impact patterns (Fig. 8a and b). Both types of El Niño produce a dry-north, wet-south anomaly pattern, similar to the seesaw pattern that has traditionally been used to describe the El Niño impacts on US winter precipitation. However, the dry anomalies produced by the CP El Niño are of larger magnitudes and cover larger areas than those produced by the EP El Niño. For example, the dry anomalies cover only the Great Lakes region during the

EP El Niño, but extend southwestward through the Ohio-Mississippi Valley toward the Gulf Coast during the CP El Niño. In contrast, the wet anomalies tend to have smaller magnitudes during the CP El Niño than during the EP El Niño—a phenomenon that appears most obviously over the Southeast US. Figs. 8a and b together indicate that the CP El Niño tends to intensify the dry anomalies but weaken the wet anomalies of the impact pattern produced by the EP El Niño. This important difference is clearly revealed in Fig. 8c, where the precipitation anomalies regressed with the EP El Niño were subtracted from the anomalies regressed with the CP El Niño (i.e., Fig. 8b minus Fig. 8a). The negative values in Fig. 8c indicate that a shift in El Niño from the EP type to the CP type makes the dry anomalies drier over the Pacific Northwest and along the Ohio-Mississippi Valley and the wet anomalies less wet over the Southeast. Southern California and Arizona are the only regions where the CP El Niño makes the winter climate wetter than during the EP El Niño events. Overall, the regression analyses reveal that the CP type of El Niño enhances the drying effect of El Niño on US winter precipitation.

B5. <u>A case study:</u> Winter precipitations in Pacific Northwest, Ohio-Mississippi Valley, Southeast, Southwest in the major El Niño years

To further confirm the different impacts produced by the two types of El Niño, we examined US winter precipitation anomalies during individual EP and CP El Niño years over the following four regions: the Pacific Northwest, Ohio-Mississippi Valley, Southeast, and Southwest. As shown in Fig. 9, the stronger drying effect of the CP El Niño over the Pacific Northwest is obvious in the figure, which shows a mean precipitation anomaly of -4.3 mm/day for the CP El Niño years but a mean of +1.5 mm/day for the EP El Niño years. Negative anomalies also tend to occur over the Pacific Northwest more consistently during the CP El Niño years (i.e., 10 out of 13 events; 77%) than during the EP El Niño years (i.e., 4 out of 8 events; 50%). This enhanced drying tendency is also very obvious in the Ohio-Mississippi Valley. During eleven of the thirteen CP El Niño years (i.e., 85%), the winter precipitation anomalies over this region are below normal, but the percentage drops to five out of eight (63%) for the EP El Niño years. Over the Southeast, both types of El Niño

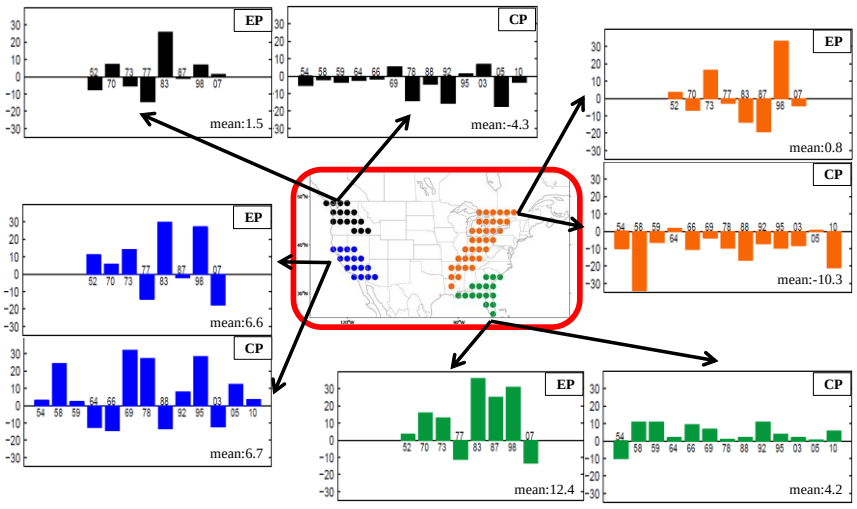

Figure 9. Winter precipitation anomalies averaged separately for the four selected US regions during the 8 major EP El Niño years and the 13 CP El Niño events. The mean anomalies averaged over the EP or CP El Niño events are also shown in the panels in unit of mm/day.

produce wet anomalies; however the precipitation anomalies are very large (with a mean value of +12.4 mm/day) during the EP El Niño winters, but are consistently small during the CP El Niño winters (with a mean value of +4.2 mm/day). Over the Southwest region, there are indications of a stronger wetting effect produced by the CP El Niño than by the EP El Niño, but the differences are not as significant as those found in the other three regions.

B6. Why enhanced winter drying during CP El Niño: A southward-displacement of jet stream

Winter precipitation over the US is primarily associated with winter storms, whose paths across the US are controlled by the locations of tropospheric jet streams. The climatological locations of the jet streams in the winter can be identified by the local maxima in the mean zonal winds at 300mb (U_{300mb}), which is found to be characterized by a double-jet feature over the west coast that merges into a single-jet over the East Coast (Fig. 10a). By analyzing the Jetstream location, we found that while both types of El Niño shift the jet streams southward from their climatological winter locations over the US (Figs. 10b and c), the shift is larger during the CP El Niño. Since the paths that winter storm moves over the US continent are steered by the jet streams, the more southward shift of the jet streams explains why the dry anomalies that El Niño typically produced over the Pacific Northwest and Ohio-Mississippi Valley expand their covering areas and increase their intensities during the CP El Niño. The more southward shifts of the jet streams are supposed to increase the storm activities and the winter precipitations over the Southwest and Southeast. However, the core of the jet streams along the eastern US moves to the Gulf during the CP El Niño (see Fig. 10c) and reduces the land area of wet anomalies over the US Southeast. The Southern end of the Southwest is the only region of the US that is exempted from the drying effect produced by El Niño when it shifts from the EP type to the CP type.

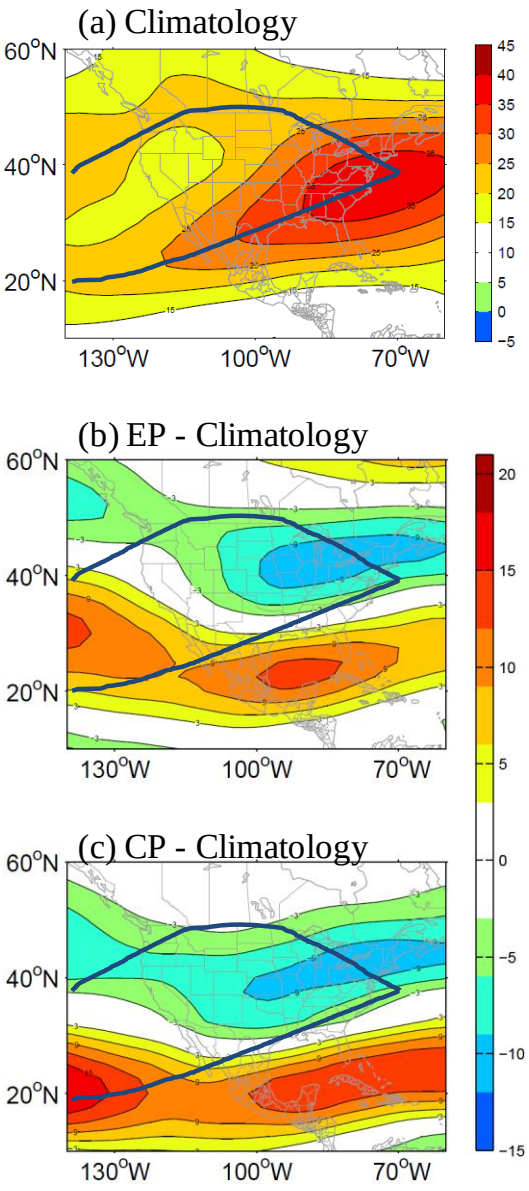

Figure 10. Winter climatological pattern of U_{300mb} (a), and the deviations from this climatology during the (b) EP El Nino and (c) CP El Nino.

B7. <u>The changing ENSO Impact on US Spring Climate</u>: An asymmetric response in *spring streamflow* to the two types of El Niño in the Mississippi River Basin

The Mississippi River Basin (MRB) occupies 41% of the contiguous U.S. and provides a vast water resource that supports the economy of the major agricultural area in North America. El Niño events play an important role in influencing the hydroclimatology over the MRB. In this study, we use statistical analyses and numerical model experiments to show that the two types of El Niño events, the CP El Niño and EP El Niño, have opposite effects on spring soil water hydrology in the MRB. Above-normal winter precipitation during EP El Niño years leads to higher soil water levels during the subsequent two to three months in the central and western MRB. On the other hand, CP El Niño events induce below-normal winter precipitation that causes lower soil water levels over the Ohio-Mississippi Valley during the following one or two months. As a result, a spring-time asymmetric response in the MRB streamflow and soil water storage to the two types of El Niño is found. Subsurface hydrological storage processes are essential to extend El Niño's influence in the MRB from winter to spring. If the CP type of El Niño occurs more frequently in the future, the overall drier land conditions and reduced river streamflow caused by the CP El Niño could pose water shortages or severe drought and threaten agricultural water supplies in the central United States.

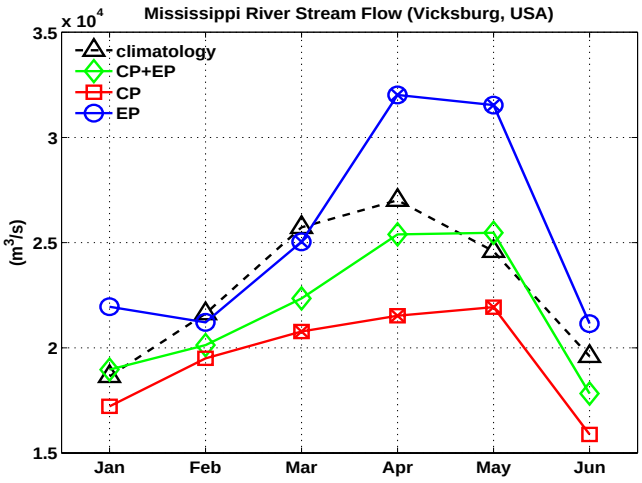

Figure 11. Monthly Mississippi River streamflow gauged at Vicksburg, USA. The climatology streamflows calculated from 1950-2006 are shown by the black line, while the streamflows are shown in red for the CP El Niño composite, in blue for the EP El Niño composite, and in green for the all-El Niño composite. An "x" within the symbol indicates that the difference in streamflow between the CP and EP El Niño composites during that month is statistically significant.

In the study, we first examined Mississippi River streamflow (at Vicksburg, Mississippi) using a global streamflow dataset. The monthly streamflow from January to June following El Niño events were composited based on seven EP El Niño and twelve CP El Niño events. The composites are shown and compared in Fig. 11 with the streamflow climatology (black). During the EP El Niño (blue), the MRB streamflow is significantly above normal after March. During the CP El Niño (red), the streamflow is below normal throughout the period, and the largest difference occurs in April, about 20% less than the climatological volume. In contrast, the largest difference during the EP El Niño occurs in May, about 28% more than the climatological value. These two types of El Niño cause the MRB streamflow to fluctuate in a range of about half of the climatological streamflow amount, which is profound. If the El Niño impact is not stratified according to the El Niño type, the streamflow composite for all the nineteen El Niño events is near or moderately below normal (see the green line in Fig. 11). This analysis indicates that a stronger and clearer impact of El Niño on the MRB streamflow can be demonstrated when the El Niño type is considered. Also, the difference in streamflow between the two types of El Niño is found to be most statistically significant during March, April, and May, indicating that impact is greatest on spring-time MRB streamflow.

Our analyses of the soil moisture storage (not shown) explain why the MRB streamflow responds differently to the two types of El Niño. During EP El Niño events, positive precipitation anomalies in late winter and early spring can penetrate to a deep layer of soil to enhance soil water storage in April and May over the central and western MRB. This two to three months lagged increase in the total soil water storage is then reflected as an increase in the MRB streamflow. On the other hand, CP El Niño events cause negative precipitation anomalies that penetrate only to a shallower layer of soil in the eastern portion of MRB with a shorter lag of 1-2 months. The decreased content in the total soil water storage then leads to reduced streamflow rate in the subsequent 1-2 months. Changes in evaporation and the snow melt can also contribute to changes in streamflow when CP and EP El Niño events occur.

B8. <u>The changing El Niño impact on the US summer climate:</u> The Great Plain Low-Level Jet

The Great Plains of the United States contributes more than 40% of the total agroeconomics in North America. The Great Plains low-level jet (GPLLJ) plays an important role in modulating the transport of heat and moisture from the Gulf of Mexico into the region during spring and summer. Fig. 12a shows the climatological values (1948-2010) of the May-June-July (MJJ) mean meridional winds at 925 hPa over the U.S. The low-level jet can be identified as the maximum in wind speeds over the Great Plains of the U.S., which also extends southward to northeastern Mexico. Variations in the strength of the GPLLJ and its associated moisture transport were also suggested to be a contributing factor for springtime tornado activity in the U.S. In this study, we stratify the El Niño influences on the GPLLJ strength according to El Niño type and find the influence is dramatically different between these two types of El Niño. The mechanisms that give rise to these different influences are also identified.

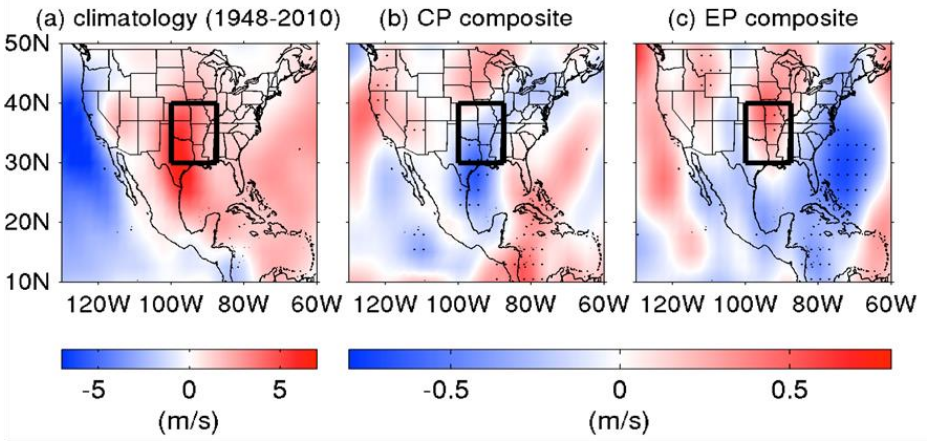

Figure 12. Meridional winds at 925 hPa during the May-June-July (MJJ) season: (a) the climatological values (1948-2010); (b) the anomalies composited from the thirteen CP El Niño events during their decaying phase; and (c) the anomalies composited from the eight EP El Niño events during their decaying phase. Statistically significant deviations are stippled. Boxes in the panels indicate the GPLLJ region, which is bounded in latitude

We performed composite analysis to show that the EP El Niño tends to increase the strength of the summer GPLLJ, which is consistent with the conventional view of El Niño's influence on the GPLLJ. However, our analysis shows that the CP El Niño tends to decrease the strength of the summer GPLLJ. During the decaying phase of the EP El Niño, the strength of the GPLLJ increases (Fig. 12c) by as much as 0.5 m/s. The strengthening of the GPLLJ is most obvious over Missouri and Arkansas, which is the northern portion of the GPLLJ. During the decaying phase of the CP El Niño (Fig. 12b), the strength of the GPLLJ decreases by about 0.5 m/s. The

decrease is particularly large over the southern portion of the GPLLJ, including Texas, Louisiana, and Arkansas. Our results indicate that the two types of El Niño produce distinct and opposite impacts on the strength of the summer-time GPLLJ.

We also find that the summer precipitation in the GPLLJ region is greatly influenced by the strength of the GPLLJ during these two types of El Niño events. As shown in Fig. 13, significant precipitation increases are found in the downwind region of the GPLLJ in May and June during the decaying phase of the EP El Niño (Fig. 13d-f), whereas significant precipitation decreases are found during the decaying phase of the CP El Niño (Fig. 13a-c). These results correspond well to the weakened (strengthened) GPLLJ, which reduces (increases) the water transport from the south to the north of Great Plains. In July, however, precipitation anomalies become positive (negative) in CP (EP) El Niño events and may be explained by local convection activities.

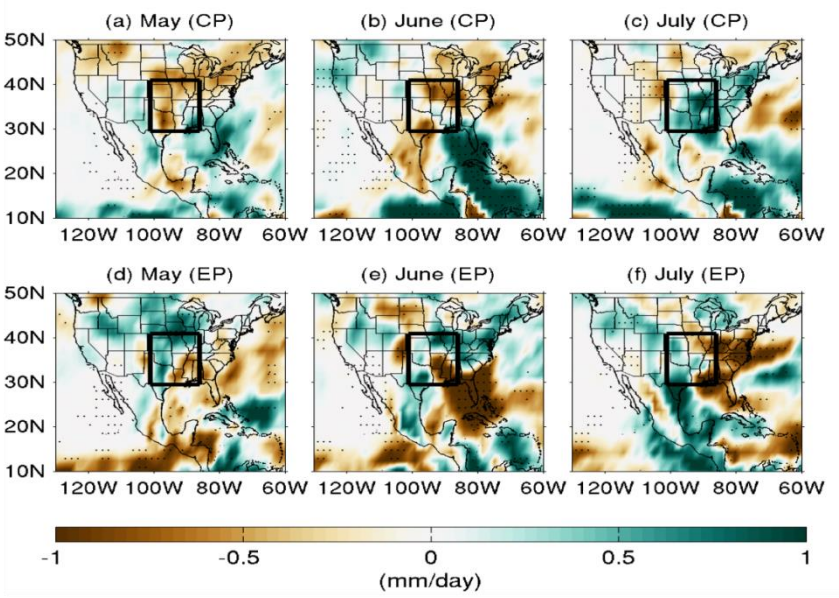

Figure 13. Precipitation anomalies during May, June, and July composted for the CP El Niño events (upper panels) and the EP El Niño events (lower panels) in their decaying phases. Statistically significant deviations are stippled.

B9. <u>The mechanisms for the changing El Niño impact on the summer GPLJ</u>

To understand why the two types of El Niño produce opposite influences on the strength of summer GPLLJ, we examined the large-scale circulation features over the U.S. during the MJJ season. Our analyses reveal that the EP El Niño increases the GPLLJ strength by producing an east-west gradient in surface air temperature that straddles the low level jet. As shown in Fig. 14, colder-than-normal temperatures are established over the Rockies (to the west of the jet), while warmer-than-normal temperatures are found over the eastern seaboard of the US. As a result of this increase in temperature gradient, southerly anomalies are produced via the thermal wind balance, enhancing the strength of the GPLLJ. Such a temperature pattern cannot be found during the CP El Niño. Instead, the CP El Niño produces significant negative sea level pressure (SLP)

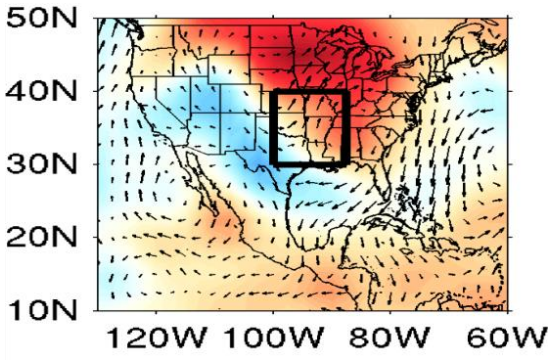

Figure 14. MJJ-mean surface air temperature anomalies and wind anomalies (vector) at 925 hPa composited from the decaying phase of the EP El Niño.

anomalies over the Gulf of Mexico. As shown in Fig. 15, the cyclonic circulation associated with this SLP anomaly produces northerly anomalies over the GPLLJ region, weakening the lowlevel jet.

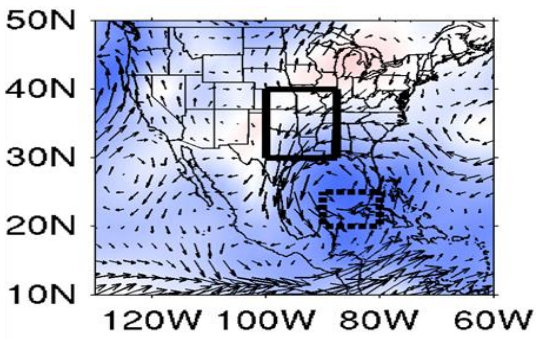

Figure 15. MJJ-mean sea level pressure anomalies (color) and 925 hPa wind anomalies (vector) composited for the (a) CP El Niño events.

This study provides evidence to show that the two types of El Niño can produce opposite impacts during their decaying phases on the strength of the GPLLJ during late spring and early summer. The finding has several implications for understanding, predicting, and projecting the U.S. summer climate. In 1988, a severe drought damaged the agroeconomics in the central U.S. and cost approximately $40.0 (61.6, adjusted to 2002 value) billion dollars. We are not aware of any studies that have attributed this drought event to the CP El Niño event occurred in 1988. Our results indicate that this CP El Niño event had the potential to contribute to the reduction in strength of the MJJ GPLLJ, which may have weakened the moisture transport from the Gulf of Mexico into the Great Plains. This may have been a contributing factor for the severe drought in 1988. Recent studies have indicated that the GPLLJ has become stronger and migrated northward since 1979, leading to an increasing trend in the precipitation in the central and northern Great Plains but a significant reduction in rainfall in the Southern Plains. GCM simulation results have suggested that global warming may amplify the GPLLJ in the future mainly due to a westward extension of a stronger North Atlantic subtropical high. Our present study suggests that the strengthening effect caused by global warming may be partially offset by the CP El Niño that has been suggested to occur more frequently in a warmer world.

C. Evaluate CMIP5 Model Performance in Simulating the Changing ENSO Impacts

C1. Using CMIP5 simulations to project the intensities of the two El Niño types in the future

We evaluated the intensity of the EP and CP types of ENSO simulated in the pre-industrial, historical, and the Representative Concentration Pathways (RCP) 4.5 experiments of the Coupled Model Intercomparison Project Phase 5 (CMIP5). Compared to the CMIP3 models, the pre-industrial simulations of the CMIP5 models are found to (1) better simulate the observed spatial patterns of the two types of ENSO and (2) have a significantly smaller inter-model diversity in ENSO intensities. The decrease in the CMIP5 model discrepancies is particularly obvious in the simulation of the EP ENSO intensity, although it is still more difficult for the models to reproduce the observed EP ENSO

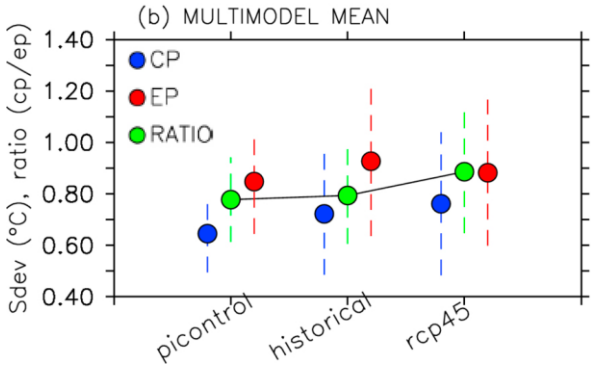

Figure 16. Multi-model mean of EP and CP intensities and the CP-to-EP ratio from the pre-industrial, historical, and RCP4.5 experiments

intensity than the observed CP ENSO intensity. Ensemble means of the CMIP5 models indicate that the intensity of the CP ENSO increases steadily from the pre-industrial to the historical and the RCP4.5 simulations, but the intensity of the EP ENSO increases from the pre-industrial to the historical simulations and then decreases in the RCP4.5 projections (Fig. 16). The CP-to-EP ENSO intensity ratio, as a result, is almost the same in the pre-industrial and historical simulations but increases in the RCP4.5 simulation. By analyzing CMIP5 simulation, we showed that both the intensity and the occurrence of the CP ENSO are projected to increase in the future warming world.

C.3 Assessing and understanding the performance of NCEP's CFS model in the simulations of the two types of ENSO

We examined the capability of the NCEP CFS model in simulating the two types of ENSO and made efforts to identify the cause of the model deficiencies. The model is found to produce both the EP and CP types of ENSO with spatial patterns and temporal evolution similar to the observed (Fig. 17). The simulated ENSO intensity is comparable to the observed for the EP type but weaker than the observed for the CP type. Further analyses reveal that the generation of the simulated CP ENSO is linked to extratropical forcing associated with the NPO and that the model is capable of simulating the coupled air-sea processes in the subtropical Pacific that slowly spreads the NPO-induced SST variability into the tropics, as shown in the observations. The simulated NPO, however, does not extend as far into the deep tropics as it does in the observations and the coupling in the model is not sustained as long as it is in the observations. As a result, the extratropical forcing of tropical central Pacific SST variability in the CFS model is weaker than in the observations. An additional analysis with the Bjerkness Stability Index (i.e., BJ Index) indicates that the weaker CP ENSO in the CFS model is also partially due to unrealistically weak zonal advective feedback in the equatorial Pacific. These model deficiencies appear to be related to an underestimation in the amount of the marine stratus clouds off the North American coasts inducing an ocean surface warm bias in the eastern Pacific. This study suggests that a realistic simulation of these marine stratus clouds can be important for the CP ENSO simulation, which we believe has never been noticed in the research community and deserves further investigations.

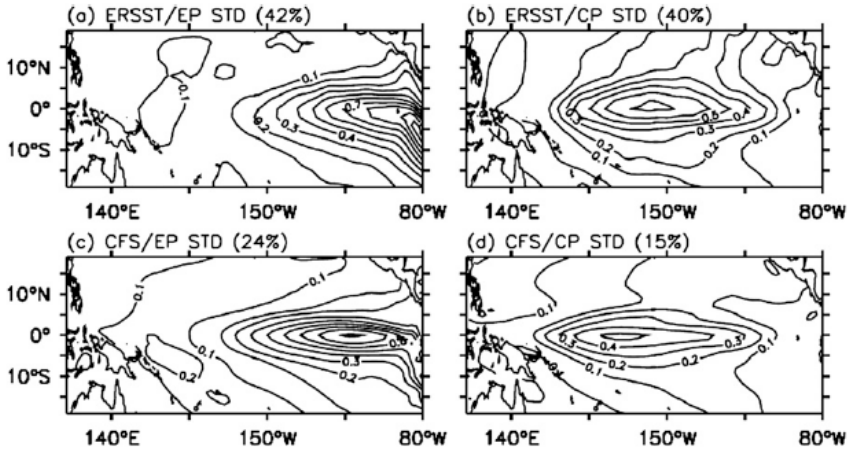

Figure 17. Spatial patterns of standard deviations (STD; unit: °C) of the first EOF mode for the (left) EP ENSO and (right) CP ENSO calculated from the observations (a, b) and CFS model (c, d). The percentage of variance explained by the first EOF mode is also shown in parentheses.

C4. CMIP5 model simulations of the changing impacts of El Niño on US winter temperature

Thirty CMIP5 preindustrial simulations were examined to conclude that the CMIP5 models can simulate the observed EP El Niño impacts realistically but not the observed CP El Niño impacts. As shown in Fig. 18a the observed US winter responses to the EP El Niño are reasonably well simulated by most of the CMIP5 models. The northeast-warm, southwest-cold pattern can be seen in many of the CMIP5 models. The pattern correlation for the "best" model is as high as 0.93 and the pattern correlations are still very high for most of the lower-ranked models. However, the situation is quite different for the CP El Niño. As shown in Fig. 18b, the pattern correlation drops quickly below 0.5 after the 9th-ranked model. The observed northwest-warm, southeast-cold pattern can only be found in the top nine "best" models. In some of the CMIP5 models, the simulated US winter responses to the CP El Niño are even opposite from the observed.

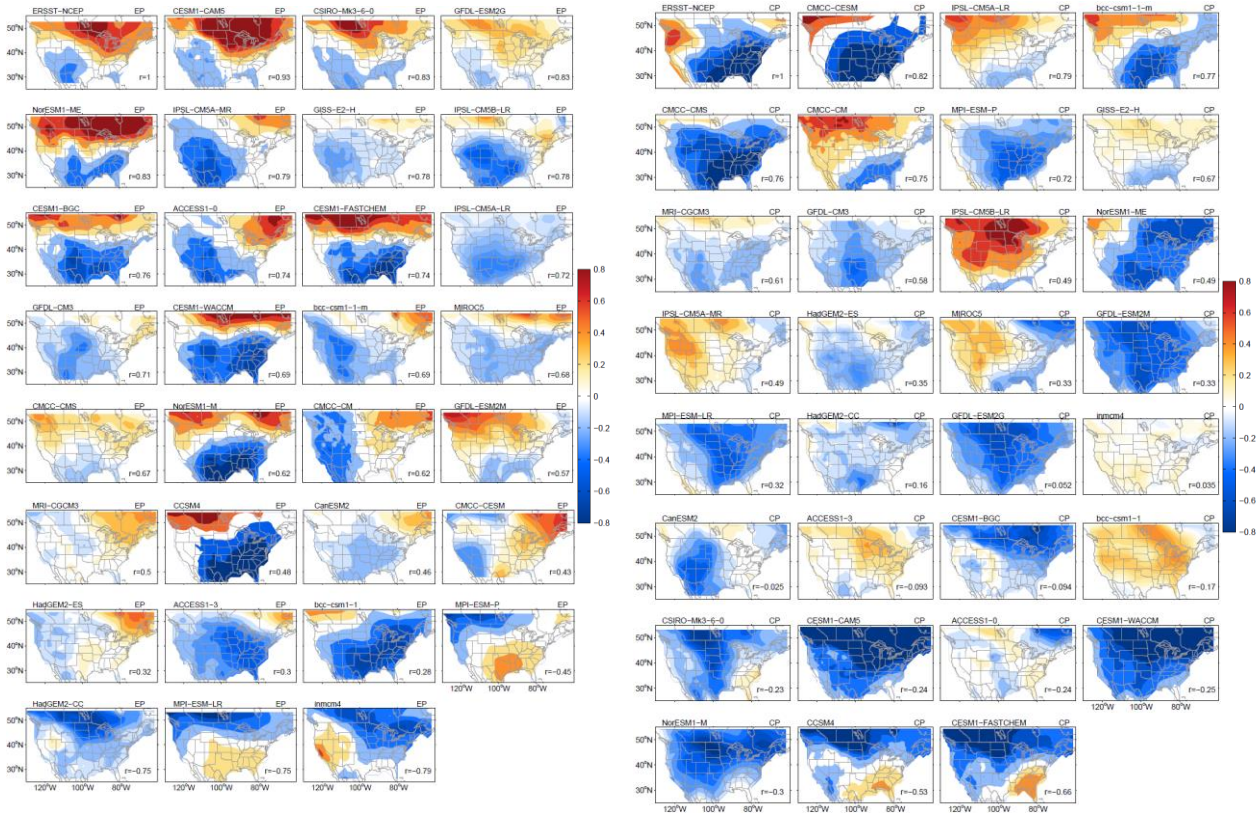

Figure 18. The US winter near-surface air temperature anomaly patterns from the observations and the thirty CMIP5 models for the (a) EP El Niño and (b) CP El Niño. The patterns are shown in units of °C. In order from the highest pattern correlation of US air temperature with observations to the lowest.

C5. Why are CMIP5 models less successful in simulating CP El Niño's impact on US?

Heating associated with deep convection is one key process by which El Niño influences the atmosphere. The intensity and location of deep convection can be represented by the outgoing longwave radiation (OLR). In order to find out why it is easier for the CMIP5 models to simulate

the US winter response to the EP El Niño than to the CP El Niño, we looked into the relationships between SST and OLR anomalies for the two types of El Niño and examine how well the observed relationships are simulated in CMIP5 models. It is found that during the EP El Niño, the largest SST anomalies are located in the eastern equatorial Pacific and can easily influence the strength of the Walker circulation to give rise to basin-wide OLR anomalies (Fig. 19a). The modeled atmospheric responses to the EP El Niño are thus not sensitive to SST anomaly structure and can be well simulated by most of the CMIP5 models. In contrast, the SST anomalies of the CP El Niño are located in the central equatorial Pacific and can induce only local OLR anomalies to the west of the SST anomalies (Fig. 19b). The modeled atmospheric responses to the CP El Niño are, therefore, different among the models depending on the simulated magnitudes and locations of the CP El Niño SST anomalies.

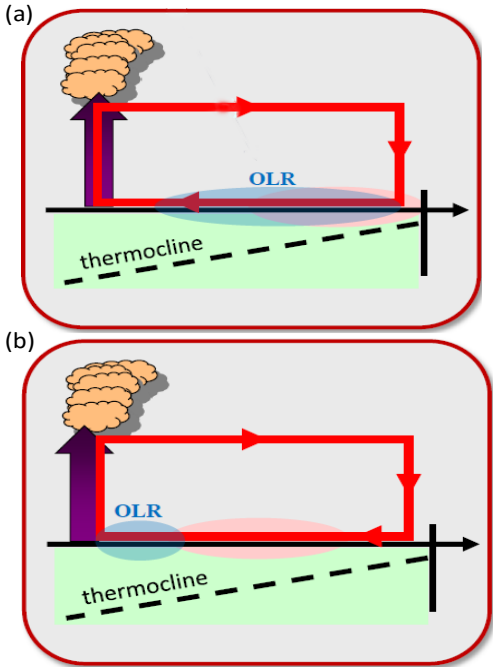

Figure 19. Schematic showing the Walker circulation, SST anomalies (pink shadings) and OLR responses (blue shadings) during (a) the EP El Niño and (b) the CP El Niño.

C6. Two distinct atmospheric wave train patterns in response to the EP and CP El Niño

Deep convective heating excites atmospheric Rossby waves that transmit El Niño influences to mid and high latitude regions including the US. The CMIP5 models are able to simulate the observed different wave train patterns generated in the extratropical atmosphere for these two types of El Niño: the Tropical/Northern Hemisphere (TNH) pattern during the EP El Niño and the Pacific-North American (PNA) pattern during the CP El Niño. While all of the CMIP5 models realistically produce a negative phase of the TNH in response to the EP El Niño and a positive phase of the PNA in response to the CP El Niño, many of the CMIP5 models also erroneously produce an incorrect phase of the TNH during CP El Niño events. The incorrect TNH response overpowers the correct PNA response in some models, leading to unrealistic simulations of the US winter response to the CP El Niño. A better understanding of the generation mechanisms of the TNH pattern and its sensitivity to the tropical Pacific heating will be required to improve the climate model simulation of the US response to the CP El Niño.

D. CP ENSO Impacts beyond the US

D.1 *Impacts on global river discharge: Mapping the locations of asymmetric and symmetric discharge responses in global rivers to the two types of El Niño*

River discharge variations play a pivotal role in global water and biogeochemical cycles and can impact the world's agro-economics. El Niño is among the factors that are known to cause interannual fluctuations in discharge in many global river basins. Previous studies have uncovered some of the El Niño-river discharge relationships. However, most of these earlier studies did not explicitly consider the existence of different types of El Niño. We have shown that the springtime Mississippi River discharge increases during EP El Niño events but decreases during CP El Niño events. We referred to these opposite signs in discharge anomalies as the "asymmetric response (AR)" to the two types of El Niño, in contrast to the "symmetric response (SR)" that would produce the same signs of anomalies during the two types of El Niño. River basins that produce the AR pattern may exhibit distinct year-to-year discharge variations in recent decades after El Niño changed from the EP to the CP type, whereas those that produce the SR pattern would be less affected by the change in El Niño type. Therefore, it is desirable to obtain an overview of which large river basins in the world produce the AR and SR patterns to the two types of El Niño. In this study, a method is developed to identify these response patterns for the world's eighteen largest rivers during the developing, mature, and decaying phases of El Niño. The major dataset used in this study is the Global River Flow and Continental Discharge Data Set.

To stratify the global river responses to the two types of El Niño, we composited the discharge anomalies for the EP and CP El Niño for each of the eighteen selected rivers. The composites use data from the May of the El Niño year (May(0)) to the July of the following year (July (1)) to cover the developing, mature, and decaying phases of El Niño events. During each phase, if the EP and CP composite anomalies are of the same sign for more than 50% of the time (three months out of five months in each phase), that river basin is regarded as producing a SR pattern to the two types of El Niño during that El Niño phase. If during 50% or more of the phase duration, the EP (CP) composite anomalies are above-normal while the CP (EP) composite anomalies are below-

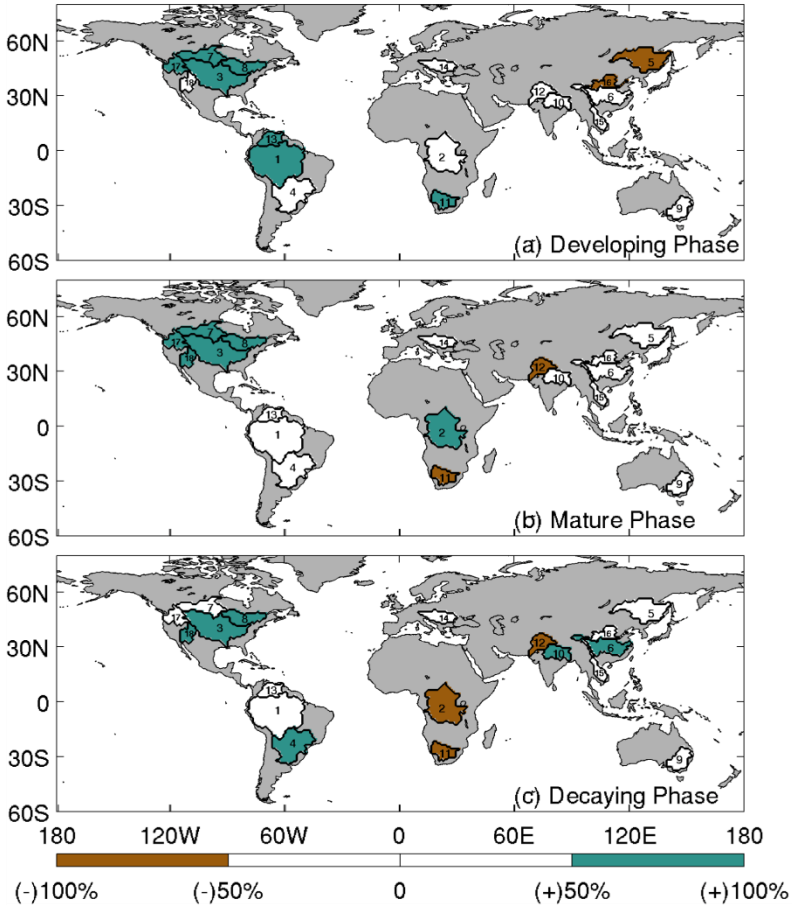

Figure 20. Discharge response patterns for global rivers during (a) the developing phase (May(0)-September(0)), (b) the mature phase (October(0)-February(1)), and (c) the decaying phase (March(1)-July(1)) of El Niño. The numbers (in unit of "%") under colorbar stand for the ratio of how many months in each phase showing an asymmetric response. The negative (positive) sign in front of the numbers indicates the AR- (AR+) response pattern.

normal, that river basin is considered to produce an AR+ (AR-) pattern.

Based on this method, we produced a global mapping (Fig. 20) to indicate the locations of world's largest river basins that produce similar response (i.e., symmetric response) or opposite response (i.e., asymmetric response) to the two types of El Niño. In the mappings, we use colors to indicate the different response patterns for the eighteen selected rivers: white for SR, green for AR+, and brown for AR-. These color markings offer a quick way to grasp the global distribution of different response patterns. From the color marking, we notice that large rivers in North America tend to produce above-normal discharge during the EP type of El Niño but below-normal discharge during the CP type (i.e., AR+ patter; green color in Fig. 20). This asymmetric response pattern indicates that El Niño type is important to the discharge variations for most of the large rivers in North America.

In South America, Fig. 20 shows that the response pattern is also relatively simple. Most of the rivers exhibit the AR+ pattern (green) in the developing phase and the SR pattern (white; except Parana River basin) for the rest of the El Niño lifecycle. These color markings indicate that the El Niño type should be considered for the South American rivers only in the developing phase. For large rivers in Europe (for example the Danube) and Australia (for example the Murray), the SR pattern persists throughout all three El Niño phases. Apparently, river discharge anomalies in these two continents are not sensitive to the El Niño type. The response patterns are more complicated for rivers in the Asian and African continents, which tend to vary not only during different phases of the El Niño lifecycle but also from river to river within the same continent.

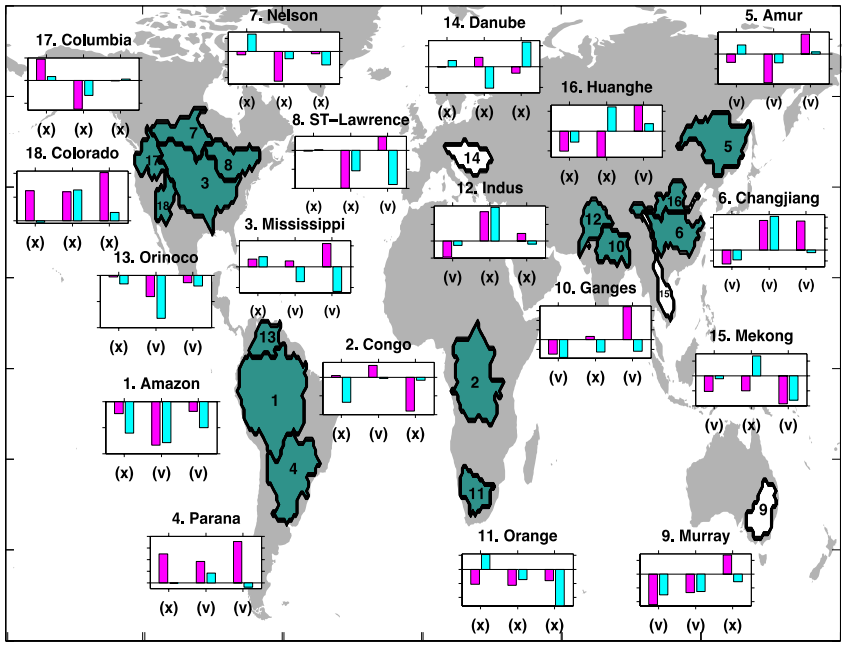

Figure 21. Composite precipitation anomalies for the EP (pink bars) and CP (light blue bars) El Niño during their developing (left-most pair of the bars), mature (middle pair), and decaying phases (right-most pair). The bar shows precipitation anomalies, calculated by averaging precipitation anomalies in each phase and normalized by its climatological value over the river basin. The "(√)" check indicates that the sign of precipitation anomalies matches the sign of the discharge anomalies, whereas the "(x)" check indicates that the signs do not match. River basins that produce the AR (SR) pattern are colored green (white).

Precipitation has been identified as the major freshwater input into a river basin. To examine the possible relationship between precipitation and discharge anomalies during the developing, mature, and decaying phases of El Niño, Fig. 21 displays the normalized and seasonally-averaged

precipitation anomalies in each river basin separately for the two types of El Niño. When the signs of precipitation anomalies match the signs of discharge anomalies for both types of El Niño in one phase, we give that phase a "(√)" symbol. Otherwise, a "(x)" symbol is given. Examining the symbols in Fig. 21, we find nine rivers showing consistent discharge and precipitation variations during at least two phases of El Niño. For these rivers, the discharge response patterns can be mostly explained by the precipitation anomalies within the river basins during the two types of El Niño. These nine rivers are: the Amazon, Amur, Changjiang, Ganges, Orinoco, Parana, Mekong, Mississippi, and Murray. It is worth noting that this group includes almost all the largest-drainage rivers in every continent, such as the Mississippi for North America, the Amazon for South America and the Changjiang for East Asia. Due to their large drainage areas, it is reasonable that their discharge variations have strong linkages to the variations in precipitation falling within the river basins.

In this study, the global distributions of the asymmetric and symmetric responses of river discharge to the EP and CP types of El Niño during their developing, mature and decaying phases are mapped for the first time. A few conclusions can be drawn from this work. Firstly, it is found that the discharge response patterns tend to be geographically dependent. Large rivers in the American continents show more persistent and simple response patterns throughout the various phases of the El Niño lifecycle, whereas rivers in Asia and Africa show complex response patterns that vary from river to river and from phase to phase. Rivers in Europe and Australia, on the other hand, produce similar discharge responses to the two types of El Niño. These general features in the mapping indicate that the El Niño type needs to be taken into consideration to understand, predict, and manage the discharge variations for the rivers in North and South America, Asia, and Africa, but not for the rivers in Europe and Australia. Secondly, local precipitation variations within the river basins are the primary factor determining the discharge response pattern for rivers that have large drainage areas. For the rivers with smaller drainage areas, the discharge response patterns cannot be explained solely by local precipitation variations. Other factors, such as land hydrological processes, need to be invoked.

Since the El Niño has changed from the EP to the CP type in the early 1990s, the mapping produced from this study offers an overview of which global rivers may have experienced changes in their discharge variation patterns during the past two decades and may need new or different strategies to project and manage their discharge in the coming decades if the CP type of El Niño continues to dominate. The five largest river basins in the North America are found to be among those river basins, which include the Mississippi, Nelson, ST-Lawrence, Columbia, and Colorado River basins.

D2. An innovative method to constrain the 21st-century warming pattern using the observed change in El Niño type

As a heat engine of the global atmosphere, the equatorial Pacific Ocean has profound impacts on precipitation, circulation, and energy transport in both climate variability and change. Large uncertainties exist in the projections made within the CMIP3 or CMIP5 ensemble for the future warming pattern in this region. While some models project a warming extending to the central Pacific, others indicate a warming located more in the eastern Pacific. There are a number of ongoing efforts to find methods to constrain the future warming projections and reduce the inter-

model uncertainty. Existing observational datasets are too short for the anthropogenic global warming signal to stand out from natural variability. However, they are adequate to examine the interannual variability in the equatorial Pacific. We developed a way to constrain the climate models' projections using the observed change in El Niño type.

We analyzed eighteen CMIP5 RCP 4.5 simulations to show that the centennial warming pattern (i.e., SST projected for the last decade of the 21st century minus the projected SST in the first decade of the century) in the equatorial Pacific can be influenced by the relative strengths of the Walker and Hadley circulations. A stronger Walker circulation is associated with stronger surface warming in the eastern equatorial Pacific via the Bjerknes feedback mechanism, while a stronger Hadley circulation with stronger change in the central equatorial Pacific through the Wind-Evaporation-SST feedback mechanism. The influences of these two atmospheric circulations on the location of the centennial warming were shown to be similar to those found for the EP and CP types of El Niño. This similarity was explored as a methodology to use the observed El Niño activity to constrain the projections of the 21st-century warming patterns. Using the observed frequency ratio of the EP and CP El Niño near the beginning of the 21st century as the constraint, we determined that the "most-likely" centennial warming in the 21st century (Fig. 22a) is characterized by weaker warming throughout the southeastern subtropicl Pacific, stronger warming in the eastern equatorial Pacific, and alternating stronger and weaker warming in the subtropical North Pacific. The mean of all the eighteen CMIP5 models (Fig. 22b) is consistent with the "most-likely" projection for the southeastern subtropical Pacific. However, it misses the finer-scale fluctuations in the subtropical North Pacific and overestimates the warming in the eastern equatorial Pacific. Our constraint method indicates that caution should be exercised when using the multi-model mean to infer future warming patterns in these two regions.

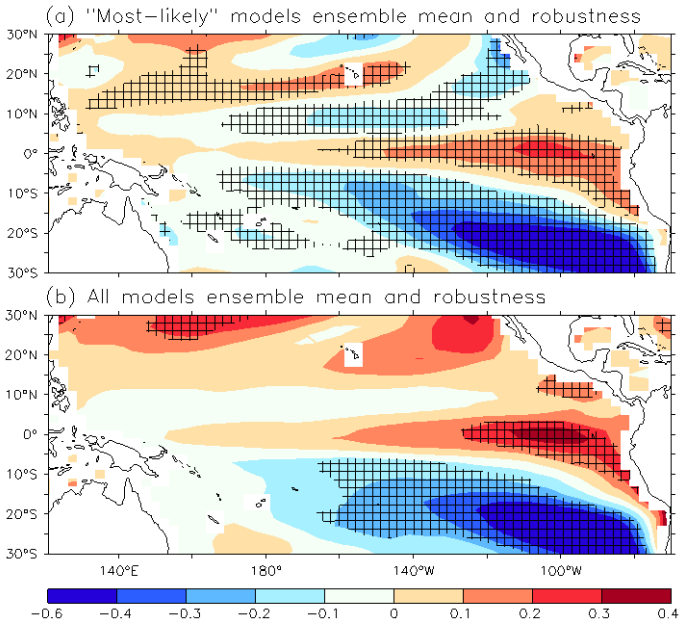

Figure 22. Ensemble mean of tropical Pacific centennial warming patterns (in K K^{-1}) projected along RCP4.5 by (a) the four "most-likely" CMIP5 models and (b) all the eighteen models.

D3. RCP4.5 projections of future changes of monsoon circulation and rainfall

North American monsoon is one of the major climate/weather phenomena important to the water supplies in the US. As part of our contribution to the MAPP CMIP5 Task Force, we analyze the CMIP5 RCP4.5 simulations to understand the future monsoon changes in the 21st century. We

noticed a "paradox" in the strength of the South Asian summer monsoon (SASM) and decided to investigate it. Since the Asian monsoon and North American monsoon owe their generation to the same basic dynamics, the understandings obtained from this study are applicable to the projection of North American Monsoon changes in the 21st century.

It is known that enhanced land-sea thermal contrasts can enhance the SASM circulation, while the "mean advection of stratification change" (MASC) mechanism tends to reduce any type of tropical circulation, including the SASM. In order to examine these mechanisms, we look into the intermodel relationship between the changes of zonal winds at the surface/upper level and land-sea thermal contrast/MASC in eighteen (18) CMIP5 RCP4.5 simulations. From this analysis, we clarify the paradox in the SASM circulation change by competing mechanisms: weakened upper tropospheric winds via the MASC effect and strengthened lower tropospheric and surface winds by the enhanced surface land-sea thermal contrast. Fig. 23 summarizes these effects by showing the vertical profiles of climatology and change of the SASM zonal wind and wind speed averaged in the SASM region and among the 18 CMIP5 RCP4.5 simulations. In fact, barotropically, the zonal wind change appears to be westerly, with two peaks at 850 hPa and 250 hPa, indicating the maximum effects of land-sea contrast and MASC, respectively. The uncertainty range marked by ensemble mean ±1 standard deviation shows that the sign of the SASM circulation change profile is robust among the models. However, because of the baroclinic nature of the climatological SASM circulation, the anomalous westerlies weaken the upper tropospheric easterly winds but strengthen the lower tropospheric westerly winds. As clearly shown by the wind speed change, the apparent paradox in the SASM circulation change is created, with the tipping point at 450 hPa.

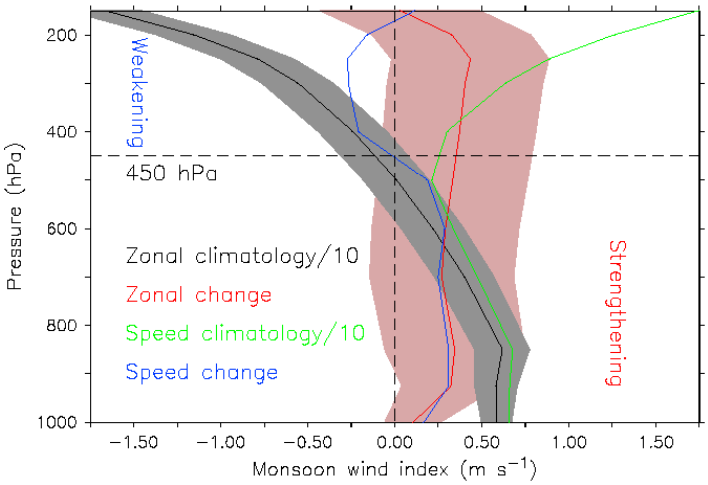

Figure 23. Ensemble and JJA mean vertical profiles of the climatological change of SASM zonal wind and wind speed indices (0°–30°N, 70°–110°E) in the RCP4.5 simulations in the 18 CMIP5 models. Shadings mark the uncertainty (±1 standard deviation) of the zonal wind.

Our moisture budget analysis (not shown) unsurprisingly suggests no significant contribution of the upper level circulation reduction to the SASM rainfall change due to low moisture content, and the precipitation change pattern can be attributed to both the moisture content increase and lower level wind enhancement leading to a total spatial mean precipitation increase, along with a tropical mean SST increase.

HIGHLIGHTS OF ACCOMPLISHMENTS

What Causes the Increased Occurrence of CP ENSO

- By analyzing the CFSv2 reanalysis, we conclude that the recent emergence of the CP El Niño is caused by the increased influence of the North Pacific Oscillation on the tropical Pacific since 1990. The nature of the El Niño has changed around 1990 from the being tropically excited to extratropical excited.
- Our investigations reveal that the recent emergence of the Central Pacific El Niño is a Pacific Ocean response to the phase change of the Atlantic Multi-decadal Oscillation (AMO).
- This AMO phase shift triggered a series of air-sea interaction in the Pacific to give rise to the Central-Pacific type of El Niño.
- Northern Hemisphere climate, including the US climate, experienced a shift in the early 1990s, which is related a switch of the AMO to its positive phase.

The Changing ENSO Impacts on US Winter Climate

- Using statistical analysis, numerical model experiments, and case studies, we show that while the conventional EP El Niño affects winter temperatures primarily over the Great Lakes, Northeast, and Southwest US, the recent shift to a greater frequency of occurrence of the CP type has made the Northwest and Southeast the regions of the US most influenced by El Niño.
- The impact of El Niño on US winter precipitation is found to have changed in association with the recent shift of the El Niño type. The emerging CP El Niño intensifies the drying effect typically produced by the traditional EP El Niño during US and is one contributing factor to the recent prevalence of extended droughts in the US.

The Changing ENSO Impact on US Spring Climate

- The emerging CP El Niño produces an opposite effect on the spring streamflow in the Mississippi River Basin (MRB) from the traditional EP El Niño, which may result in more frequent water shortages in the Mississippi River Basin.
- Subsurface hydrological storage processes are found to be essential to extend El Niño's influence in the MRB from winter to late spring.
- The overall drier land conditions and reduced river streamflow caused by the CP El Niño could pose water shortages, threatening agricultural water supplies in the central United States.

The Changing ENSO Impact on US Summer Climate

- The weakening effect on the Great Plain Low Level Jet (GPLLJ) by the emerging CP El Niño during the summer time is in contrast to the strengthening effect for the conventional EP type.
- The EP El Niño strengthens the GPLLJ by inducing a zonal temperature gradient across the GPLLJ region, while the CP El Niño weakens the GPLLJ by inducing a surface cyclonic circulation anomaly over the Gulf of Mexico.

CMIP5 Simulations of the Changing ENSO Impact on US Climate

- By analyzing CMIP5 simulations, we project that both the intensity and the occurrence of the CP ENSO are expected to increase in the future warming world.
- By analyzing CMIP5 pre-industrial simulations, we find that it is more difficult for climate models to accurately simulate the El Niño impacts on US winter climate after the El Niño shifts from its traditional EP type to the new CP type. The model deficiency resides on the simulation of the Tropical North Hemisphere (TNH) wave train pattern in the extratropcial atmosphere, which has been overlooked in the past studies.
- We demonstrate that the NCEP's CFS model is more capable of simulating the EP type of ENSO than simulating the CP type of ENSO. Improving the simulation of the California marine stratus is one promising area of model improvements that can further improve the model performance in ENSO simulation.

The Changing ENSO Impact beyond the US

- A global mapping has been produced to locate which global rivers may have experienced changes in their discharge variation patterns during the past two decades and may need new or different strategies to project and manage their discharge in the coming decades if the CP type of El Niño continues to dominate.
- The five largest river basins in the North America (i.e., the Mississippi, Nelson, ST-Lawrence, Columbia, and Colorado River basins) are among the river basins that produce the asymmetric response pattern to the two types of El Niño, for which new strategies are needed to project and manage their discharge in the coming decades.
- The El Niño type needs to be taken into consideration to understand, predict, and manage the discharge variations for the rivers in North and South America, Asia, and Africa, but not for the rivers in Europe and Australia.
- Local precipitation variations within the river basins are the primary factor determining the discharge response pattern for rivers that have large drainage areas.
- An innovative method is developed to constraint the 21st century warming patterns using the observed change in the El Niño type. The method enables us to identify a "most-likely" warming pattern projected by CMIP5 models for the 21st century. This method can be further used to identify the "most-likely" projection of the future change on North America climate.
- The future changes in the monsoon (including the Southeast Asia monsoon and the North American monsoon) circulation and rainfall in a warming world will be determined not only by changes in the surface land-sea thermal contrast but also by changes in the mean advection of stratification change mechanism.

PUBLICATIONS ACKNOWLEDGED THE SUPPORT FROM THIS PROJECT

(1) Liang, Y.-C., J.-Y. Yu, M.-H. Lo, and C. Wang, 2015: The Changing Influence of El Niño on the Great Plains Low-Level Jet, *Atmospheric Science Letters*, DOI: 10.1002/asl.590.

(2) Wang, C., C. Deser, J.-Y. Yu, P. DiNezio, and A. Clement, 2015: El Niño and Southern Oscillation (ENSO): A Review, A Chapter for Springer Book: Coral Reefs of the Eastern Pacific, In Press.

(3) Yu, J.-Y., P.-K. Kao, H. Paek, H.-H. Hsu, C.-W. Hung, M.-M. Lu, S.-I. An, 2015: Linking Emergence of the Central-Pacific El Niño to the Atlantic Multi-decadal Oscillation, *Journal of Climate*, **28**, 651-662, doi: 10.1175/JCLI-D-14-00347.1.

(4) Yu, J.-Y. and H. Paek, 2015: Precursors of ENSO beyond the tropical Pacific, *US CLIVAR Variations*, Winter 2015 Issue, Vol. 13, No. 1, 15-20.

(5) Yu, J.-Y., X. Wang, S. Yang, H. Paek, and M. Chen, 2015: The Changing El Niño Southern Oscillation, Book Chapter in Climate Extremes: Patterns and Mechanisms, Wang, S.-Y., J.-H. Yoon, C. Funk, and R. R. Gillies (Ed.), AGU Monograph, Accepted.

(6) Capotondi, A., A. T. Wittenberg, M. Newman, E. Di Lorenzo, J.-Y. Yu, P. Braconnot, J. Cole, B. Dewitte, B. Giese, E. Guilyardi, F.-F. Jin, K. Karnauskas, B. Kirtman, T. Lee, N. Schneider, Y. Xue, S.-W. Yeh, 2014: Understanding ENSO diversity, *Bulletin of the American Meteorological Society*, **96**, 921-938, doi:10.1175/BAMS-D-13-00117.1.

(7) Liang, Y.-C., M.-H. Lo, and J.-Y. Yu, 2014: Asymmetric Responses of Land Hydroclimatology to Two Types of El Niño in the Mississippi River Basin, *Geophysical Research Letters*, **41**, 582-588, doi:10.1002/2013GL058828.

(8) Ma, J. and J.-Y. Yu, 2014: Linking Centennial Surface Warming Patterns in the Equatorial Pacific to the Relative Strengths of the Walker and Hadley Circulations, *Journal of Atmospheric Sciences*, **71**, 3454-3464, doi: 10.1175/JAS-D-14-0028.1.

(9) Ma, J. and J.-Y. Yu, 2014: Paradox in South Asian summer monsoon circulation change: Lower tropospheric strengthening and upper tropospheric weakening, *Geophysical Research Letters*, doi: 10.1002/2014GL059891.

(10) Qian, C., J.-Y. Yu, G. Chen, 2014: Decadal Summer Drought Frequency in China: The increasing influence of the Atlantic Multi-decadal Oscillation, *Environmental Research Letters,* **9**, 124004, doi:10.1088/1748-9326/9/12/124004.

(11) Zheng, F., X.-H. Fang, J.-Y. Yu, and J. Zhu, 2014: Asymmetry of the Bjerknes Positive Feedback between the Two Types of El Niño, *Geophysical Research Letters*, **41**, 7651-7657, doi:10.1002/2014GL062125

(12) Zou, Y., J.-Y. Yu, T. Lee, M.-M. Lu, and S. T. Kim, 2014: CMIP5 Model Simulations of the Impacts of the Two Types of El Niño on US Winter Temperature, *Journal of Geophysical Research*, **119**, 3076-3092, doi: 10.1002/2013JD021064.

(13) Sheffield, J. and co-authors, 2013: North American Climate in CMIP5 Experiments. Part II: Evaluation of 20th Century Intra-Seasonal to Decadal Variability, *Journal of Climate*, **23**, 9247-9290, doi: 10.1175/JCLI-D-12-00593.1.

(14) Yu, J.-Y. and S. T. Kim, 2013: Identifying the Types of Major El Niño Events since 1870, *International Journal of Climatology*, **33**, 2105-2112. doi: 10.1002/joc.3575.

(15) Yu, J.-Y. and Y. Zou, 2013: The enhanced drying effect of Central-Pacific El Niño on US winter, *Environmental Research Letters*, **8**, doi:10.1088/1748-9326/8/1/014019.

(16) Kim, S. T., J.-Y. Yu, and M.-M. Lu, 2012: Distinct Behaviors of Pacific and Indian Ocean Warm Pool Properties on Seasonal and Interannual Timescales, *Journal of Geophysical Research*, **117**, D05128, doi: 10.1029/2011JD016557

(17) Kim, S. T., J.-Y. Yu, A. Kumar, and H. Wang, 2012: Examination of the Two Types of ENSO in the NCEP CFS Model and Its Extratropical Associations, *Monthly Weather Review*, **140**, 1908-1923, doi: 10.1175/MWR-D-11-00300.1.

(18) Kim, S. T. and J.-Y. Yu, 2012: The Two Types of ENSO in CMIP5 Models, *Geophysical Research Letters*, **39**, L11704, doi:10.1029/2012GL052006.

(19) Yu, J.-Y., Y. Zou, S. T. Kim, and T. Lee, 2012: The Changing Impact of El Niño on US Winter Temperatures, *Geophysical Research Letters*, doi:10.1029/2012GL052483.

(20) Yu, J.-Y., M.-M. Lu, and S. T. Kim, 2012: A change in the relationship between tropical central Pacific SST variability and the extratropical atmosphere around 1990, *Environmental Research Letters*, *7*, doi:10.1088/1748-9326/7/3/034025.